

Physicochemical and Mechanical Properties of Gelatin Reinforced with Nanocellulose and Montmorillonite

Mercedes Echegaray¹, Gurutz Mondragon¹, Loli Martin², Alba González³, Cristina Peña-Rodríguez¹ and Aitor Arbelaiz^{1*}

¹Materials+Technologies Group, Engineering College of Gipuzkoa, Pza. Europa 1, 20018, University of the Basque Country (UPV/EHU), Donostia-San Sebastián, Spain

²Macrobehaviour-Mesostructure-Nanotechnology, General Research Service (SGIker), University of the Basque Country (UPV/EHU), Donostia-San Sebastián, Spain

³Department of Polymer Science and Technology, Faculty of Chemistry, Institute for Polymer Materials (POLYMAT), University of the Basque Country, P.O. Box 1072, 20080 San Sebastián, Spain

Received January 18, 2016; Accepted March 30, 2016

ABSTRACT: Organic rodlike cellulose nanocrystals extracted from sisal fibers and inorganic montmorillonite based on silicate layers were employed to develop bionanocomposites based on gelatin matrix. Bionanocomposites with cellulose nanocrystal, montmorillonite and both nanoreinforcements combined were characterized by Fourier transform infrared spectroscopy, thermogravimetric analysis and differential scanning calorimetry. Tensile properties and oxygen and water vapor gas permeability values were determined to study the influence of the addition of nanoreinforcements, different in nature, to gelatin matrix. Bionanocomposites with montmorillonite improved tensile strength but systems reinforced with nanocellulose showed lower tensile strength than neat gelatin ones. Oxygen gas permeability values decreased for all bionanocomposites, especially for montmorillonite systems; however, after the incorporation of reinforcements water vapor permeability increased.

KEYWORDS: Barrier properties, gelatin, montmorillonite, nanocellulose

1 INTRODUCTION

Biopolymers obtained from natural sources are interesting materials to reduce the dependence on fossil sources [1]. Gelatin, obtained from the partial hydrolysis of collagen, has been one of the most used biopolymers throughout history and is composed mainly of proteins, minerals, salts and water [2, 3]. Gelatin is an amphoteric polyelectrolyte macromolecule and $-NH_2$ and $-COOH$ functional groups can be found in molecular chains. These functional groups can be ionized depending on the gelatin isoelectric point and the pH media used. Gelatin presents good barrier properties against oxygen and aromas in low and intermediate relative humidity [4]. In addition, gelatin is biodegradable and has excellent biocompatibility. Nevertheless, gelatin has some drawbacks [5, 6] which necessitate the modification of biopolymer to

have the appropriate properties to use in packaging. The mechanical and permeability properties need to be improved. Due to the exceptional properties of cellulose nanocrystals (CNC), the addition of rodlike crystalline cellulose with high aspect ratio, high surface area and high crystallinity, could be the way to improve the properties of gelatin [6–8]. To isolate CNC from sisal fibers, firstly non-cellulosic components must be removed, maintaining cellulose crystalline structure. Then, an acid hydrolysis must be performed to isolate the crystalline fraction [9–11]. However, as observed in a previous work [6], although the oxygen transmission rate decreased after the addition of 5 and 10 wt% of CNC to gelatin, the water vapor transmission rate increased.

Several matrices have been modified by the incorporation of inorganic clays [5, 12–15]. In different works it was observed that the addition of montmorillonite (MMT) to gelatin resulted in materials with improved water vapor barrier properties [12, 14–16]. Montmorillonite is an inorganic clay mineral consisting

*Corresponding author: aitor.arbelaiz@ehu.es

of silicate layers which are nontoxic, cheap and show high aspect ratio.

The aim of this work is to develop bionanocomposites based on gelatin matrix and nanoreinforcements such as CNC and MMT, and their combinations. For comparison purposes, nanocomposites based on 5 and 10 wt% of both CNC and MMT were prepared. By this comparison, the effect of the reinforcement nature and structure on the final material properties was studied. On the other hand, with the aim of obtaining gelatin based materials with improved gas barrier properties, gelatin/CNC/MMT nanocomposites were prepared. The obtained materials have been characterized in order to determinate their physical, chemical and mechanical properties.

2 EXPERIMENTAL

2.1 Materials

Acid pretreated commercial gelatin powder (G) type A from pigskin with an isoelectric point (IEP) of 7, purchased by Sigma, was employed as received. Cellulose nanocrystals were extracted from the sisal fibers using the same procedure described in a previous work [9]. Montmorillonite was purchased by Southern Clay Products, Inc. (Cloisite-Na⁺) and was employed as received.

2.2 Bionanocomposite Film Preparation

Bionanocomposite films based on gelatin were prepared by solvent casting method using the procedure described in a previous paper [6]. The pH values of the gelatin suspensions were around 5. In Table 1 the

Table 1 Designations and compositions of prepared systems.

Designation	Gelatin (wt%)	CNC (wt%)	MMT (wt%)
G	100	0	0
CNC1	99	1	0
CNC3	97	3	0
CNC5	95	5	0
CNC10	90	10	0
MMT5	95	0	5
MMT10	90	0	10
MMT1/CNC4	95	4	1
MMT2.5/CNC2.5	95	2.5	2.5
MMT4/CNC1	95	1	4

prepared materials and designations are summarized. Concerning bionanocomposites with montmorillonite as reinforcement, in order to separate tactoids into platelets, montmorillonite water suspension was previously sonicated for 48 h [13]. In bionanocomposites reinforced with both nanocellulose and montmorillonite, nanocellulose suspensions were added to the montmorillonite suspension and finally the gelatin was added. The thickness range of the obtained films was between 35 and 85 μm . Control gelatin films were prepared under similar conditions. Samples were conditioned at 25 °C and 50% RH in a climatic chamber (Binder KBF 115) before testing.

2.3 Bionanocomposites Characterization

Attenuated total reflection Fourier transform infrared spectra were recorded on a Nicolet Nexus 670 FTIR spectrometer equipped with a single horizontal Golden Gate ATR cell with ZnSe cell/crystal. Dumbbell shaped specimens according to ASTM D1708-93 standard [17] were tested by a MTS Insight Tester using Testwork 4.0 software equipped with a video extensometer at a crosshead speed of 1 mm/min. Oxygen transmission rate (OTR) measurements were carried out using a Mocon OX-TRAN 2/21 MH model at a pressure of 1 atm, a temperature of 23 °C and 50% relative humidity in accordance with the ASTM D3985-05 standard [18]. Water vapor transmission rate (WVTR) measurements were carried out using a permeation gravimetric cell (GPCell) at 25 °C according to ASTM E96-95 standard [19]. The water penetrant inside the cell (water activity = 1) was placed on a Sartorius balance with a readability of 10⁻⁵ g and the weight loss of the cell was monitored and recorded in a computer for further data treatment.

Two heating scans were performed from -25 to 250 °C at a heating rate of 10 °C/min using Mettler DSC822 equipment. Thermogravimetric measurements were performed by using a TGA/SDTA 851 Mettler Toledo instrument. Dynamic tests were run from 25 to 700 °C at a heating rate of 10 °C/min under nitrogen atmosphere. The distribution of nanocellulose and nanoclays in gelatin matrix was analyzed by an atomic force microscope (AFM) from Digital Instruments having a NanoScope III controller with a MultiMode head (Veeco) with an integrated silico tip/cantilever.

3 RESULTS AND DISCUSSION

3.1 FTIR Spectroscopy Results

The FTIR spectra of neat gelatin and prepared bionanocomposites are shown in Figures 1 and 2. The spectrum of gelatin displayed various characteristic

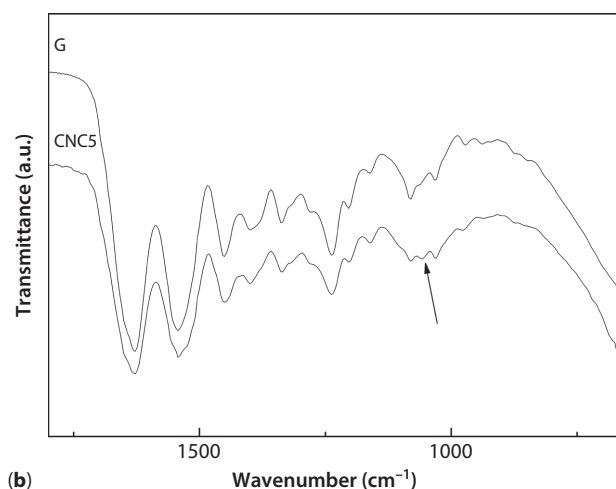
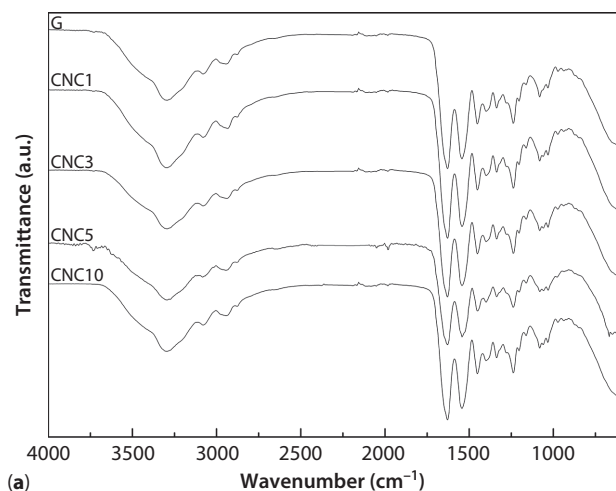


Figure 1 Fourier transform infrared spectra of neat gelatin and bionanocomposite films: (a) with different CNC contents and (b) magnified region.

bands in the range from 750 to 4000 cm^{-1} . Amide A was related to the N-H stretching vibration of hydrogen bonded amide groups at 3600–3200 cm^{-1} . In addition to the amide A band, in the same region, the O-H stretching vibration band of water molecules appeared [6]. A band appeared at 2935 cm^{-1} , which corresponded to the C-H stretching mode. The bands appeared at 1629, 1543 and 1234 cm^{-1} , corresponding to amide I, amide II and amide III, respectively. The intense band at 1629 cm^{-1} was related to carbonyl (C=O) stretching/hydrogen bonding coupled with COO. The band appearing at 1543 cm^{-1} is associated with the bending vibration of N-H group. The bands from 1451 to 1239 cm^{-1} were related to C-N and N-H stretching vibrations [20]. After the addition of both reinforcements, slight changes were observed in the shape of the band situated at 3500–3000 cm^{-1} , which seemed to indicate the occurrence of hydrogen

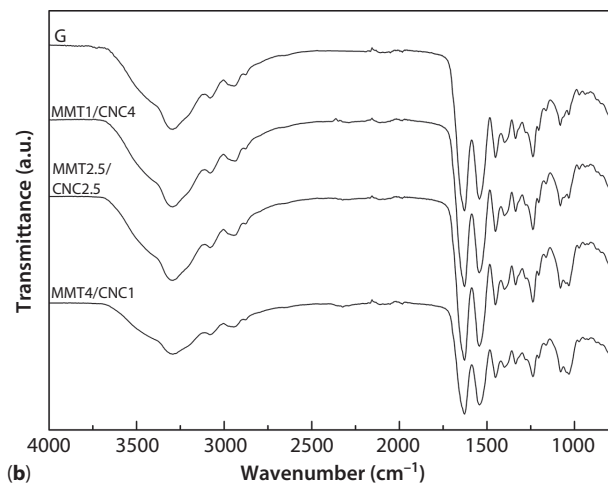
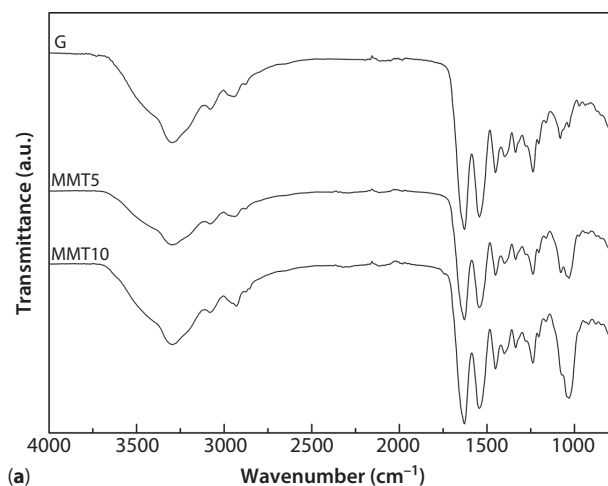


Figure 2 Fourier transform infrared spectra of neat gelatin and bionanocomposite films: (a) with different MMT contents and (b) with different CNC/MMT ratios.

bonding interactions between gelatin groups (amino, hydroxyl and carboxylic) and reinforcement hydroxyl groups (Figures 1 and 2). In addition, the intensity of the band at 1048 cm^{-1} increased in all spectra, which can be related to the presence of cellulose [6]. By the application of the second derivative procedure the shift of absorption bands and intensity changes were more clearly observed. The band at 1546 cm^{-1} related to $\delta_{\text{N-H (Sciss)}}$, $\nu_{\text{C-H}}$ [21], after MMT incorporation shifted to 1538 cm^{-1} , indicates the occurrence of interactions between structural groups of clay and gelatin chain groups. The intensity of the band at 1045 cm^{-1} was increased as MMT content was increased in bionanocomposites; this band was related to the stretching mode vibration of Si-O [22]. In nanocomposites reinforced with both reinforcements, CNC and MMT, the shape of the band situated at 3500–3000 cm^{-1} changed and the band at 1546 cm^{-1} also shifted to 1538 cm^{-1} .

3.2 Thermostability Analysis

The TGA curves of neat gelatin and bionanocomposites are shown in Figure 3. Two main weight losses were observed, the first one between 30 and 180 °C is related to water evaporation (almost 12%). This result is in agreement with previous works [4, 6] where water content of gelatin-based systems observed was between 8 and 12%. The second weight loss between 220 and 620 °C could be associated with gelatin degradation [4, 6] and the temperature of maximum degradation of gelatin being around 327 °C. In Table 2 some TGA data for neat gelatin and bionanocomposites are reported. It was observed that the degradation of neat gelatin started at 277 °C. The addition of nanoreinforcements seemed to slightly increase the thermal stability of gelatin. According to Panzavolta *et al.* [5] the presence of clay provoked a delay in the second weight loss corresponding to decomposition of the protein.

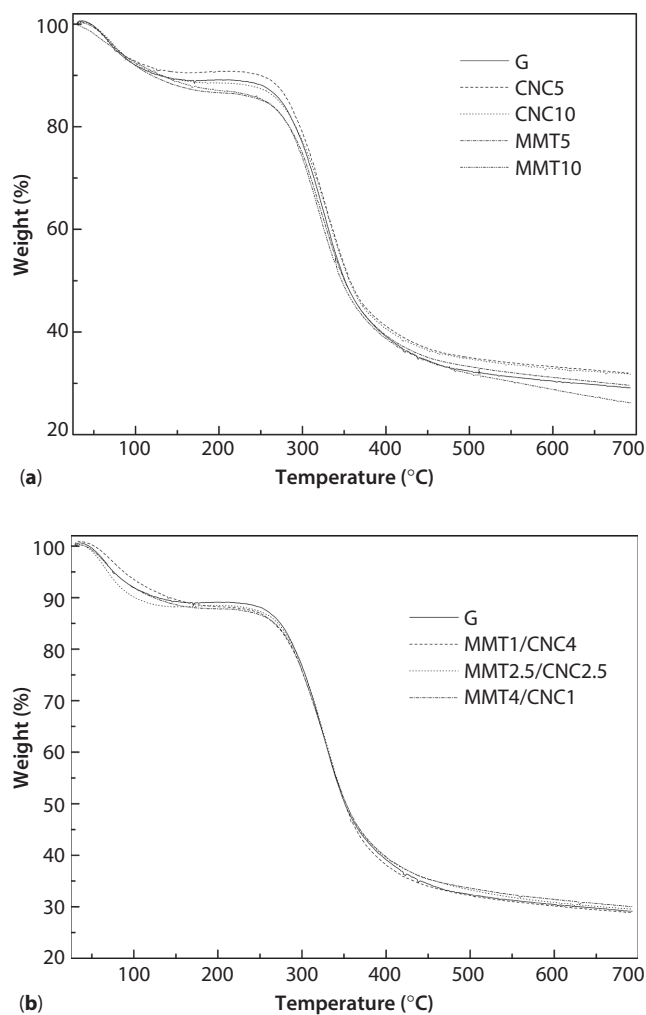


Figure 3 Thermogravimetric curves of neat gelatin and bionanocomposite films: (a) with different CNC and MMT contents and (b) with different CNC/MMT ratios.

The thermal parameters obtained from DSC first and second heating scans for gelatin and bionanocomposites are shown in Table 3. In the first scan an endothermic peak appeared between 20 and 190 °C, which was related to water evaporation and melting of the triple-helix structure of gelatin [5, 6, 23, 24], and another endothermic peak around 224 °C, which could be due to other transition in gelatin. Gelatin T_g cannot be seen because water evaporation and helix-coil transition processes could interfere with the detection of the glass transition temperature [6]. After the first heating scan water was removed and in the second heating scan neat gelatin showed T_g at 207 °C.

When the amount of water present in gelatin was increased, T_g shifted at lower temperatures [25]. In general, after the incorporation of nanoreinforcements the T_g values observed were similar or slightly higher than neat gelatin ones. Regarding the systems that contain

Table 2 Main thermal degradation data obtained by thermogravimetric analysis of neat gelatin and bionanocomposites.

System	T_{onset} (°C)	T_{max} (°C)	Char at 600 °C (%)
G	277	327	29
CNC5	278	327	32
CNC10	280	331	32
MMT5	281	319	30
MMT10	285	324	26
MMT1/CNC4	278	330	29
MMT2.5/CNC2.5	280	327	30
MMT4/CNC1	279	329	30

Table 3 Main DSC thermal data of gelatin and bionanocomposites.

System	1 st scan		2 nd scan
	$T_{\text{first peak}}$ (°C)	$T_{\text{second peak}}$ (°C)	T_g (°C)
G	95	224	207
CNC5	100	226	209
CNC10	99	226	209
MMT5	100	226	207
MMT10	98	227	207
MMT1/CNC4	98	224	204
MMT2.5/CNC2.5	102	225	207
MMT4/CNC1	95	227	211

cellulose nanocrystals, the interaction between gelatin and nanocellulose molecules might be enhanced without water [6].

3.3 Mechanical Properties

Tensile properties of neat gelatin and bionanocomposites are shown in Figure 4. Taking into account the thickness of obtained films, the elongation at break of bionanocomposites were similar or slightly higher than neat gelatin. In the literature it was observed that as the nanocellulose content was increased in bionanocomposites, the elongation at break decreased [6, 26]. After the addition of CNC to gelatin matrix the tensile strength decreased, suggesting that there is a poor adhesion between gelatin and nanocellulose. In a previous work [6] SEM micrographs of CNC-reinforced gelatin matrix suggested that there was a lack of adhesion between

nanocrystals and gelatin matrix, which is in agreement with the results reported in this work. A possible explanation could be that gelatin and CNC could create some hydrogen bonds, as observed in FTIR results, which seemed not to be enough to create a strong CNC/gelatin adhesion. Neat gelatin has a modulus value of around 4 GPa and bionanocomposites reinforced with cellulose nanocrystals showed lower or similar moduli values. In systems reinforced with MMT, the elongation at break was inversely proportional to the montmorillonite content [5, 16]. Nevertheless, after the addition of MMT the strength and moduli values increased with respect to neat gelatin. Furthermore, the strength and moduli values increased as the nanoclay content was increased in nanocomposites. Nanocomposites showed improved tensile strength, probably due to stronger interfacial adhesion between MMT and gelatin matrix. Panzavolta *et al.* [5] studied the

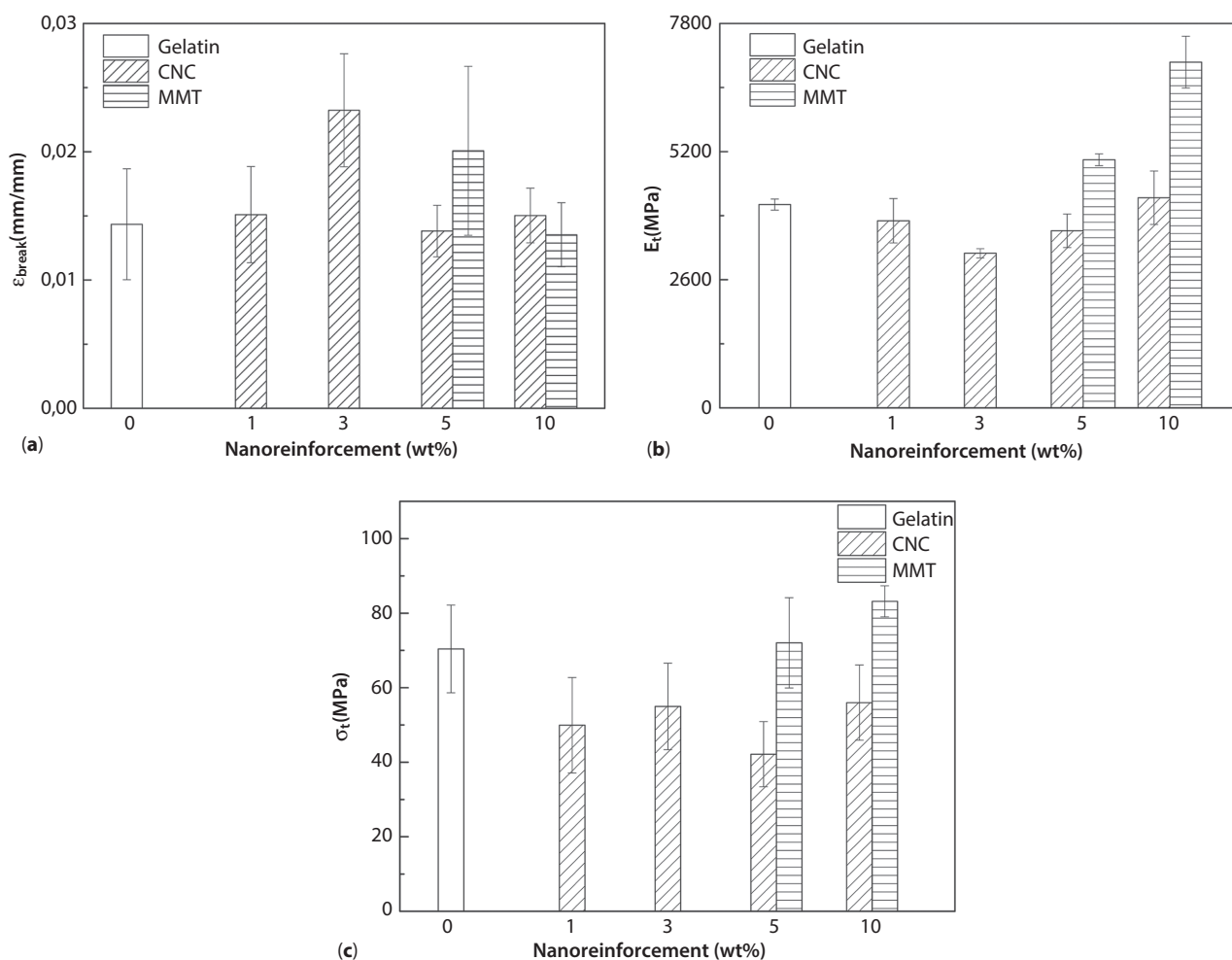


Figure 4 Tensile properties of neat gelatin and bionanocomposites based on CNC and MMT: (a) elongation at break, (b) modulus and (c) strength.

mechanical properties of type A gelatin/montmorillonite nanocomposites. They observed that prepared gelatin solutions display pH values below the isoelectric point and they suggested that the biopolymer was positively charged, enhancing interaction with the negatively charged clay sheets. In our work, bionanocomposites were prepared in $\text{pH} < \text{IEP}$; therefore, gelatin NH_2 groups would be ionized into NH_3^+ form. Formed NH_3^+ ions could create strong electrostatic interactions with MMT layers, which could be the reason for the displacement of the gelatin band from 1546 cm^{-1} to 1538 cm^{-1} after MMT incorporation. Ferfera-Harrar and Dairi [21] suggested that

at $\text{pH} < \text{IEP}$, the gelatin chains rich in NH_3^+ groups could interact with negatively charged MMT layers. Hence, they concluded that an efficient MMT intercalation was reached via electrostatic interactions which were stronger than hydrogen bond interactions developed in the case of basified gelatin systems [21]. Tensile properties of bionanocomposites reinforced with both CNC and MMT are shown in Figure 5. The moduli and strength values increased as the amount of MMT was increased. This result can be explained by taking into account the different types of interactions created by CNC and MMT with gelatin matrix.

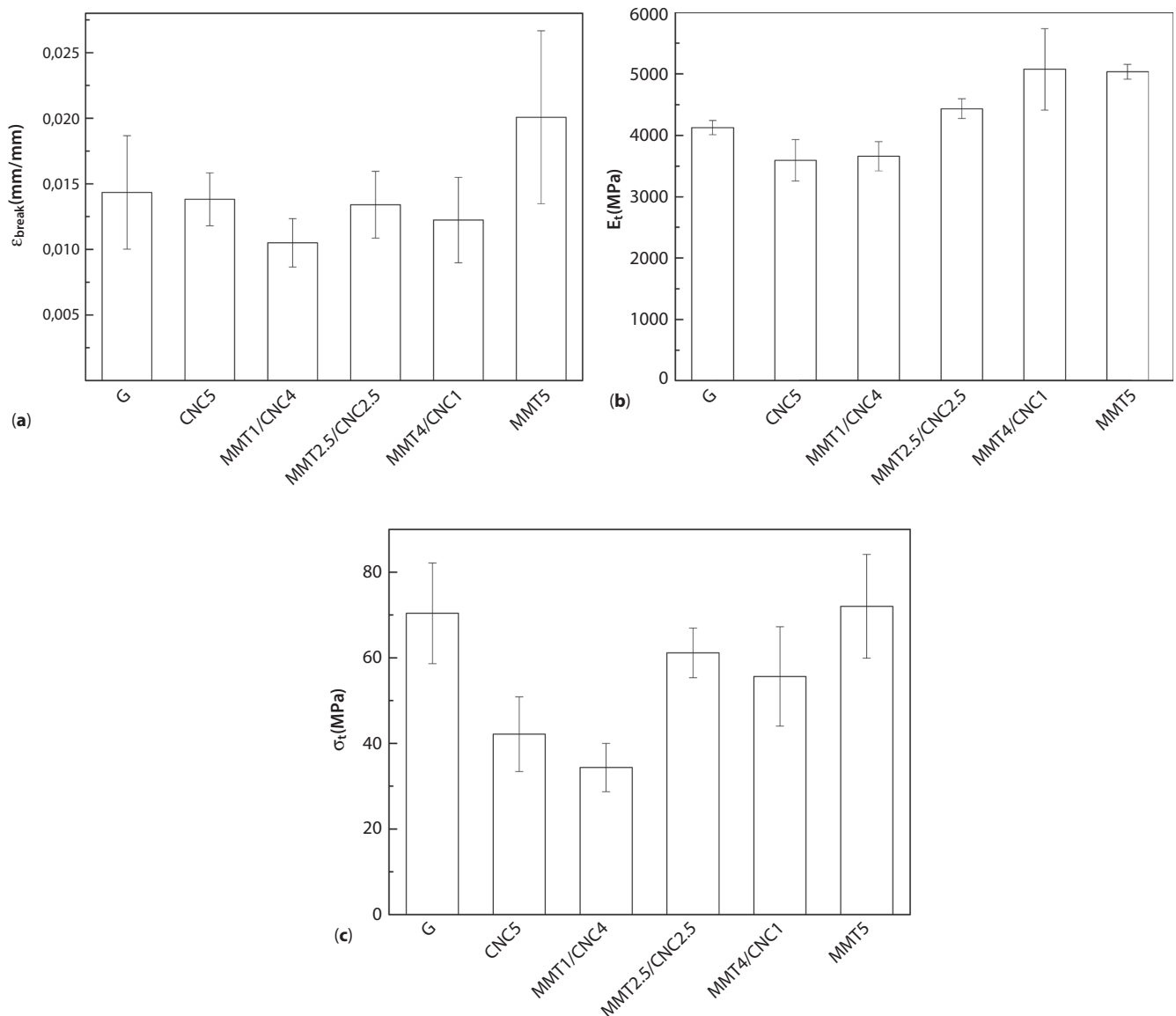


Figure 5 Tensile properties of neat gelatin and bionanocomposites based on different CNC/MMT ratios: (a) elongation at break, (b) modulus and (c) strength.

Table 4 Oxygen transmission rate values of neat gelatin and bionanocomposites.

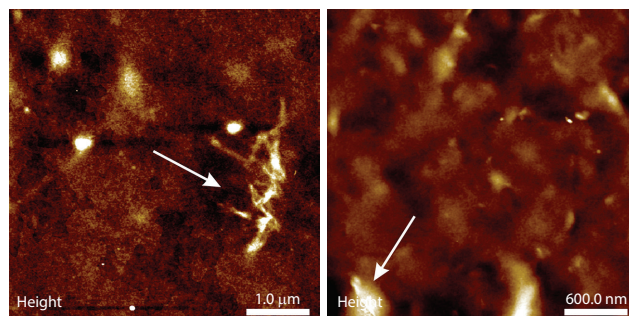
System	Thickness (μm)	OTR (cc mm/m ² day atm)
G	61.7 \pm 11.0	0.37 \pm 0.01
CNC5	52.6 \pm 3.0	0.20 \pm 0.10
CNC10	76.5 \pm 9.8	0.28 \pm 0.01
MMT5	81.3 \pm 10.3	0.09 \pm 0.03
MMT10	49.6 \pm 13.7	0.06 \pm 0.01
MMT1/CNC4	72.9 \pm 9.2	0.37 \pm 0.05
MMT2.5/CNC2.5	54.6 \pm 8.5	0.19 \pm 0.03
MMT4/CNC1	66.3 \pm 26.5	0.12 \pm 0.02

Table 5 Water vapor transmission rate values of neat gelatin and bionanocomposites.

System	Thickness (μm)	WVTR (g mm/m ² day)
G	49.1 \pm 6.4	82.6 \pm 13
CNC5	63.2 \pm 4.4	107.2 \pm 9.2
CNC10	60.7 \pm 5.7	94.2 \pm 7.5
MMT5	79.4 \pm 15.5	116.5 \pm 19
MMT10	65.1 \pm 19.7	79.7 \pm 19
MMT1/CNC4	37.5 \pm 14.5	57.4 \pm 15
MMT2.5/CNC2.5	61.5 \pm 1.2	91.6 \pm 1.3
MMT4/CNC1	82.9 \pm 4.0	129.5 \pm 8.7

3.4 Oxygen Vapor and Water Vapor Permeability

Oxygen gas and water vapor permeability of neat gelatin and bionanocomposites were determined and the values are reported in Tables 4 and 5. Bionanocomposites showed lower OTR values than neat gelatin; especially MMT-reinforced systems showed a remarkable reduction in the permeability values. This fact seemed to be due to MMT could create a tortuous pathway for oxygen diffusion [20], improving barrier property. Obtained results are in agreement with the values reported by Bae *et al.* [16]. They observed a reduction in OTR value of around 75% after 9 g of clay were added to 100 g of gelatin. Voon *et al.* [27], using the casting method, prepared bovine gelatin-based bionanocomposite films with halloysite nanoclay as reinforcing material. They observed that the WVTR value of gelatin decreased about \sim 20% after the addition of halloysite nanoclay but this decrease was statistically nonsignificant. They indicated that halloysite could exhibit minimal

**Figure 6** AFM images of gelatin bionanocomposites based on (a) CNC and (b) MMT.

dispersion in bovine gelatin matrix, leading to an ineffective and inadequate tortuous path for the diffusion of water molecules through the film matrix.

Except for nanocomposite based on MMT1/CNC4 blend, after the incorporation of reinforcements WVTR values increased. Although gelatin/MMT systems seemed to show stronger interfacial adhesion than gelatin/CNC ones, in terms of WVTR values there was no significant difference between both systems. As water has a plasticizing effect in gelatin, in WVTR testing water vapor could probably reduce gelatin matrix T_g and the system might change from a glassy state to a rubbery state. Probably all WVTR values reported are for a rubbery state and reinforcements addition to gelatin matrix has no significant impact on WVTR values [6]. On the other hand, in agreement with our results, Voon *et al.* [27] observed that the addition of nanoclay to bovine gelatin resulted in higher tensile strength but they did not observe a significant decrease of water vapor permeability.

In the AFM image of nanocomposite based on gelatin and cellulose nanocrystal (Figure 6a), CNC agglomeration can be clearly seen (see arrow). On the other hand, although AFM images of nanocomposite based on gelatin and clay revealed an even distribution of the nanoclay particles in the gelatin matrix (Figure 6b), agglomeration of some particles was also evidenced (see arrow).

4 CONCLUSIONS

Gelatin-based bionanocomposites were obtained using CNC and MMT reinforcements. The shape of the band situated at 3500–3000 cm^{-1} changed after the addition of reinforcements, which could indicate the occurrence of hydrogen bonding interactions between gelatin groups (amino, hydroxyl and carboxylic) and reinforcement hydroxyl groups. On the other hand, by the application of the second derivative procedure,

after MMT addition to gelatin the band at 1546 cm^{-1} shifted to 1538 cm^{-1} , indicating the occurrence of interactions between structural groups of clay and gelatin chain groups. Bionanocomposites with nanocellulose showed lower tensile strength than neat gelatin, suggesting a poor stress transfer from the matrix to the nanocellulose. Nevertheless, bionanocomposites with montmorillonite improved tensile strength, probably due to the stronger interfacial adhesion between MMT and gelatin matrix. Oxygen gas permeability values decreased for all bionanocomposites, especially for MMT systems in which the clay dispersion was better than CNC ones. However, after the incorporation of reinforcements WVTR values increased. The addition of nanoreinforcements slightly increased the thermal stability of gelatin.

ACKNOWLEDGMENTS

Financial support from the Basque Country Government in the frame of Grupos Consolidados (IT-776-13) and Elkartek 2015 FORPLA3D project is gratefully acknowledged. Moreover, technical and human support provided by SGIker (UPV/EHU, MINECO, GV/EJ, ERDF and ESF) is also gratefully acknowledged.

REFERENCES

1. Y. Zhou, M. Fan, L. Chen, and J. Zhuang, Lignocellulosic fibre mediated rubber composites: An overview. *Compos. Part B Eng.* **76**, 180–191 (2015).
2. A. Duconseille, T. Astruc, N. Quintana, F. Meersman, and V. Sante-Lhoutellier, Gelatin structure and composition linked to hard capsule dissolution: A review. *Food Hydrocoll.* **43**, 360–376 (2015).
3. R. Schrieber and H. Gareis, *Gelatin Handbook: Theory and Industrial Practice*, Wiley-VCH (2007).
4. P. Kanmani and J. Rhim, Physicochemical properties of gelatin/silver nanoparticle antimicrobial composite films. *Food Chem.* **148**, 162–169 (2014).
5. S. Panzavolta, M. Giofrè, B. Bracci, K. Rubini, and A. Bigi, Montmorillonite reinforced type A gelatin nanocomposites. *J. Appl. Polym. Sci.* **131**, 40301–40306 (2014).
6. G. Mondragon, C. Peña-Rodríguez, A. Gonzalez, A. Eceiza, and A. Arbelaiz, Bionanocomposites based on gelatin matrix and nanocellulose. *Eur. Polym. J.* **62**, 1–9 (2015).
7. D. Dehnada, Z. Emam-Djomehb, H. Mirzaeia, S. Jafaria, and S. Dadashi, Optimization of physical and mechanical properties for chitosan–nanocellulose biocomposites. *Carbohydr. Polym.* **105**, 222–228 (2014).
8. S. Karimi, A. Dufresne, P. Md. Tahir, A. Karimi, and A. Abdulkhani, Biodegradable starch-based composites: Effect of micro and nanoreinforcements on composite properties. *Mater. Sci.* **49**, 4513–4521 (2014).
9. G. Mondragon, S. Fernandes, A. Retegi, C. Peña-Rodríguez, I. Algar, A. Eceiza, and A. Arbelaiz, A common strategy to extracting cellulose nanoentities from different plants. *Ind. Crop. Prod.* **55**, 140–148 (2014).
10. O. Kristiina, and S. Mohini (Eds.), *Cellulose Nanocomposites: Processing Characterization and Properties*, vol. 938, ACS Symposium Series, American Chemical Society (2005).
11. A.N. Frone, D.M. Panaitescu, and D. Donescu, Some aspects concerning the isolation of cellulose micro- and nano-fibers. *U.P.B. Sci. Bull., Series B* **73**, 133–152 (2011).
12. P. Kanmani and J. Rhim, Physical, mechanical and antimicrobial properties of gelatin based active nanocomposite films containing AgNPs and nanoclay. *Food Hydrocoll.* **35**, 644–652 (2014).
13. M. López, M. Blanco, A. Vazquez, N. Gabilondo, A. Arbelaiz, J.M. Echeverría, and I. Mondragon, Curing characteristics of resol-layered silicate nanocomposites. *Thermochim. Acta* **467**, 73–79 (2008).
14. A. Farahnaky, S.M.M. Dadfar, and M. Shahbazi, Physical and mechanical properties of gelatin–clay nanocomposite. *J. Food. Eng.* **122**, 78–83 (2014).
15. H.J. Bae, D.O. Darby, R.M. Kimmel, H.J. Park, and W.S. Whiteside, Effects of transglutaminase-induced cross-linking on properties of fish gelatin–nanoclay composite film. *Food Chem.* **114** 180–189 (2009).
16. H.J. Bae, H.J. Park, S.I. Hong, Y.J. Byun, D.O. Darby, R.M. Kimmel, and W.S. Whiteside, Effect of clay content, homogenization RPM, pH, and ultrasonication on mechanical and barrier properties of fish gelatin/montmorillonite nanocomposite films. *Food Sci. Tech.* **42**, 1179–1186 (2009).
17. Standard test method for tensile properties of plastics by use of microtensile specimens, ASTM D1708-93 (1993).
18. Standard test method for oxygen gas transmission rate through plastic film and sheeting using a colorimetric sensor, ASTM D3985-10 (2010).
19. Standard test methods for water vapour transmission of materials, ASTM E96-95 (1995).
20. P. Kanmani and J. Rhim, Physical, mechanical and antimicrobial properties of gelatin based active nanocomposite films containing AgNPs and nanoclay. *Food Hydrocoll.* **35**, 644–652 (2014).
21. H. Ferfera-Harrar and N. Dairi, Green nanocomposite films based on cellulose acetate and biopolymermodified nanoclays: Studies on morphology and properties. *Iran Polym. J.* **23**, 917–931 (2014).
22. A. Vazquez, M. López, G. Kortaberria, L. Martín, and I. Mondragon, Modification of montmorillonite with cationic surfactants. Thermal and chemical analysis including CEC determination. *Appl. Clay Sci.* **41**, 24–36 (2007).
23. W. Ma, C.-H. Tang, S.-W. Yin, X.-Q. Yang, Q. Wang, F. Liu, and Z.-H. Wei, Characterization of gelatin-based edible films incorporated with olive oil. *Food Res. Int.* **49**, 572–579 (2012).
24. P.J.A. Sobral and A.M.Q.B. Habitante, Phase transitions of pigskin gelatin. *Food Hydrocoll.* **15**, 377–382 (2001).
25. M.-F. Pinhas, J.M.V. Blanshard, W. Derbyshire, and J.R. Mitchell, The effect of water on the physicochemical

- and mechanical properties of gelatin. *J. Thermal Anal.* **47**, 1499–1511 (1996).
26. J.G. Siddaramaiah, High performance edible nano-composite films containing bacterial cellulose nanocrystals. *Carbohydr. Polym.* **87**, 2031–2037 (2012).
27. H.C. Voon, R. Bhat, A.M. Easa, M.T. Liong, and A.A. Karim, Effect of addition of halloysite nanoclay and SiO₂ Nanoparticles on barrier and mechanical properties of bovine gelatin films. *Food Bioprocess Technol.* **5**, 1766–1774 (2012).